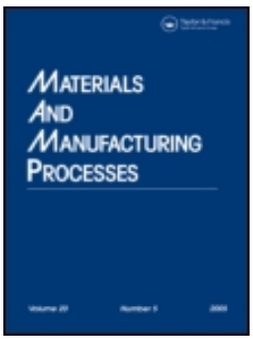

Materials and Manufacturing Processes

ISSN: 1042-6914 (Print) 1532-2475 (Online) Journal homepage: https://www.tandfonline.com/loi/lmmp20

Influence of Die Angle on Containerless Extrusion of Commercially Pure Titanium Tubes

K. Srinivasan & P. Venugopal

To cite this article: K. Srinivasan & P. Venugopal (2007) Influence of Die Angle on Containerless Extrusion of Commercially Pure Titanium Tubes, Materials and Manufacturing Processes, 22:2, 238-242, DOI: 10.1080/10426910601134047

To link to this article: https://doi.org/10.1080/10426910601134047

Materials and Manufacturing Processes, 22: 238–242, 2007

ISSN: 1042-6914 print/1532-2475 online
DOI: 10.1080/10426910601134047

Taylor & Francis
Taylor & Francis Group

Influence of Die Angle on Containerless Extrusion of Commercially Pure Titanium Tubes

K. Srinivasan[1] and P. Venugopal[2]

[1]*Department of Metallurgical and Materials Engineering, National Institute of Technology Karnataka, Surathkal, Srinivasnagar, India*
[2]*Department of Metallurgical and Materials Engineering, Materials Forming Lab, Indian Institute of Technology Madras, Chennai, India*

Containerless tube extrusion has been investigated with commerically pure titanium at room temperature and a strain rate of $0.07\,s^{-1}$ using 20 conical dies of five different strains and four different angles with MoS_2 lubricant. Theoretical punch pressures have been calculated using appropriate equations from slab analysis of the process and compared with experimentally determined punch pressures. It is found that there exists an optimum angle at which the punch pressure is the least at a given strain.

Keywords Angle; Container; Die; Experimental; Extrusion; Force; Friction; Lubricant; Pressure; Stress; Temperature; Theoretical; Titanium; Tubes.

Nomenclature

A	Surface area of deformation zone
A_f	Final area of cross-section
A_0	Initial area of cross-section
C	Specific heat
Contl.e	Containerless extrusion
Conv.e	Conventional extrusion
d_{iB}	Inner diameter of hollow billet
D_{oB}	Outer diameter of hollow billet
d_{iE}	Inner diameter of extrude
D_{oE}	Outer diameter of extrude
F	Force
F_{dfr}	Die friction force
F_{id}	Ideal force
F_{sh}	Shear force
F_{mfr}	Mandrel friction force
F_{cwbfr}	Container wall billet friction force
H_0	Initial height
ID	Inner diameter of ring specimen
K	Strength coefficient
L	Length of billet in container
n	Strain hardening experiment
OD	Outer diameter of ring specimen
P_p	Punch pressure
R	Radius of container
S_y	Yield stress
ΔT_{ad}	Adiabatic temperature rise
ΔT_{dfr}	Die frictional temperature rise
ΔT_{sh}	Shear work temperature rise
ΔT_{mfr}	Mandrel frictional temperature
Δt	Time interval of extrusion
v_R	Velocity of ram
V	Volume of deformation zone

Greek Letters

α	Semi-die angle
β	0.95
ε	Strain
μ	Friction factor
σ_{fm}	Mean flow stress $= K\varepsilon^n/n+1$
σ_N	Stress normal to inclined face in the deformation zone of die
ρ	Density

Introduction

Conventional extrusion is done using a container. Containerless extrusion, also called free extrusion or open-die extrusion, is done without a container [1, 2]. It is an unconventional process, like hydrostatic extrusion. Hydrostatic extrusion requires the least force due to minimum frictional contribution to the overall force. Conventional direct extrusion requires the maximum force due to maximum frictional forces. Containerless extrusion comes in between due to the partial elimination of frictional force due to the absence of container billet friction. But die friction and mandrel friction will be present. In containerless tube extrusion frictional force reduction [3, 4] is substantial. Lubricant consumption is less. Lower capacity presses are sufficient. Surface finish will be better than conventional extrusion but there are two disadvantages. First one is due to the unsupported billet above the die. If the length-to-diameter ratio is more than three there will be Euler buckling. The second one is that of higher strain. The higher the extrusion strain the higher the forces. If the extrusion force is larger than the upsetting force, billet will deform

Received June 11, 2006; Accepted October 25, 2006
Address correspondence to Dr. K. Srinivasan, Professor, Department of Metallurgical and Materials Engineering, National Institute of Technology Karnataka, Surathkal, Srinivasnagar 575 025, India; E-mail: ksrini@nitk.ac.in

above the die causing bulging and not through the die [5] Therefore containerless extrusion is for smaller strains and shorter billets [6–8].

The variables that decide the pressure for extrusion are strain, die angle, friction coefficient, and flow stress of material [9, 10]. Here, in this study, the influence of die angle on the pressure required for containerless tube extrusion of commercially pure (CP) titanium at room temperature is highlighted.

Experimental

Axisymmetric compression test, ring compression test, and containerless tube extrusion tests were carried out on annealed CP titanium to determine the influence of die angle on punch pressure. 40 mm-diameter CP titanium rods were forged to 30 mm diameter in a double-action pneumatic hammer and then annealed at 973 K for 2 hrs. A glass coating has been used to minimize the effect of atmosphere containing N_2, O_2, and H_2.

30 mm-diameter rods were machined into billets of height $h_0 = 37.5$ mm and diameter $d_0 = 25$ mm (to give $h_0/d_0 = 1.5$) and used for compression test in a 100 T hydraulic press to characterize the flow properties. MoS_2 was used as lubricant at room temperature and at a strain rate of $0.07\,s^{-1}$. Yield stress (S_y), strength coefficient (K), and strain hardening exponent (n) are obtained from the compression test [11].

Ring samples of 24 mm outer diameter (OD), 12 mm inner diameter (ID), and 8 mm height (h_0) were machined and compressed for estimating friction factor m [12] in the same hydraulic press, at room temperature and at a strain rate of $0.075\,s^{-1}$ using the same lubricant. HCHCr cylindrical dies were used.

Containerless tube extrusion tests were carried out on hollow billets of h_0 24 mm, inner diameter $d_{iB} = 10$ mm, and outer diameter $d_{oB}36 =$ mm (to give $h_0/d_{oB} = 1.5$) in the same hydraulic press at the same temperature and same strain rate and using the same lubricant. The experimental setup for extrusion is shown in Fig. 1. Twenty conical dies were used with five strains of 0.18, 0.25, 0.35, 0.45, and 0.54 and four angles of 12, 15, 25, and 30. The shape of the die is shown in Fig. 2, and dimensions are shown in Table 1.The dies were made of quenched and double-tempered high-speed steels (18% W:4% Cr: 1% V) of hardness 50 R_c–55 R_c.

Force stroke diagrams were recorded using a load cell, Linear Voltage Differential Transducer (LVDT), six-channel amplifier and x–y recorder. Experimental punch pressures were calculated and theoretical punch pressures were estimated using slab analysis [13].

Table 1.—Details of die dimensions.

2α (degrees)	A (mm)	B (mm)	C (mm)	D (degrees)
12	22.30	12.60	13.40	6.0
15	22.30	10.00	16.00	5.0
25	22.30	6.00	20.00	5.0
30	22.30	4.90	21.10	4.5
12	21.70	16.00	10.00	6.5
15	21.70	12.70	13.30	6.0
25	21.70	7.60	18.40	4.5
30	21.70	6.30	19.70	4.4
12	20.90	19.00	7.00	11.0
15	20.90	15.20	10.80	8.4
25	20.90	9.00	17.00	5.0
30	20.90	7.50	18.50	4.6
12	20.10	23.00	3.00	20.0
15	20.10	18.40	7.60	11.0
25	20.10	10.90	15.10	5.5
30	20.10	9.00	17.00	5.5
12	19.40	26.00	1.40	30.0
15	19.40	21.20	4.80	13.4
25	19.40	12.60	13.40	6.0
30	19.40	10.40	15.60	5.2

Material: High-speed-steel hardened to 50–55 Rc.

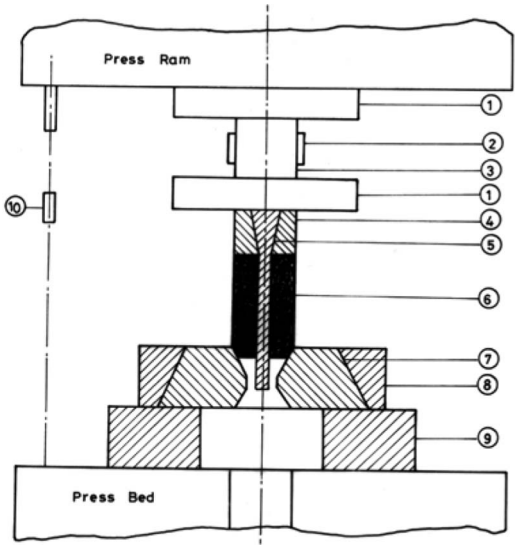

Figure 1.—Schematic experimental set up. 1. Plate, 2. Strain gauge, 3. Load cell, 4. Sleeve, 5. Mandrel, 6. Hollow billet, 7. Die ring, 8. Shrink ring, 9. Spacer block, 10. LVDT.

Results

The outcome of axisymmetric compression and ring compression tests are shown in Table 2. Force–stroke

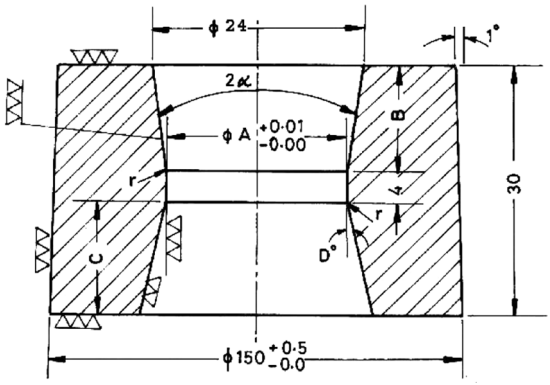

Figure 2.—Shape of the conical die. (Not to scale; all dimensions in mm.)

TABLE 2.—Flow properties.

Material	K (Mpa)	n	μ	S_y (Mpa)
CP Titanium	1100	0.34	0.14	390

diagrams are shown in Fig. 3. There is an initial rise in force due to die filling and afterwards it remains constant if containerless extrusion had taken place. If upsetting takes place force continually increases with a slope change at the point where upsetting starts.

Variation of theoretical punch pressures with die angles are shown in Fig. 4 and variation of experimental punch pressures with die angles are shown in Fig. 5 at different strains. A minimum occurs in pressure values in theoretical curves. This minimum shifts to higher angles as the strain increases, as one would expect from Fig. 6. All experimental curves decrease with angle up to 30°. Higher angles have not been used. It is expected to increase at higher angles as shown by theoretical curves. In both the figures the yield stress is shown. When punch pressure exceeds yield stress the limit of pure extrusion process occurs. The strain at which this occurs is called the limit strain.

DISCUSSION

According to slab analysis the theoretical punch pressure [13] varies with die angle as follows:

$$P_{\rho_{th}} = \sigma_{fm}[(\alpha/2) + \varepsilon(1 + (2\mu)/(\sin 2\alpha) + (A_f/A_o)(\mu/\tan\alpha))] \quad (1)$$

The optimum die angle [14] is given by

$$\cos(2\alpha)_{\text{opt}} = \left\{(-2 + c^{\varepsilon})(4\mu\varepsilon) \pm \sqrt{[(2 + c^{\varepsilon}) + 4\mu\varepsilon)]^2 + 4[1 - 4\mu\varepsilon e^{\varepsilon}]}\right\}/2 \quad (2)$$

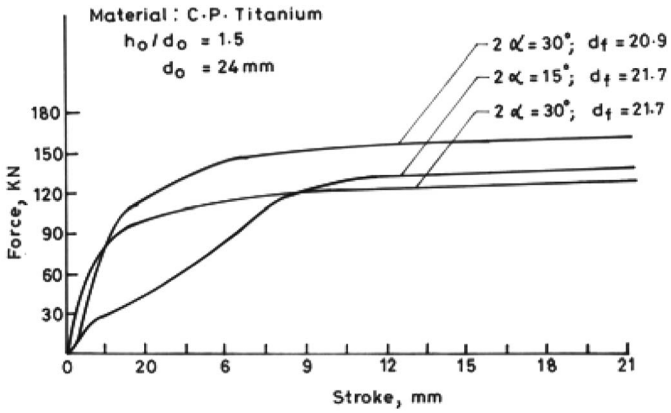

FIGURE 3.—Force–stroke diagram.

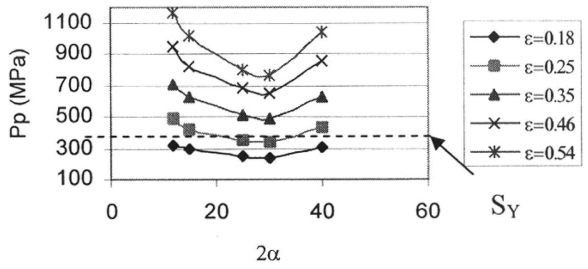

FIGURE 4.—Variation of theoretical punch pressure with angle at different strains.

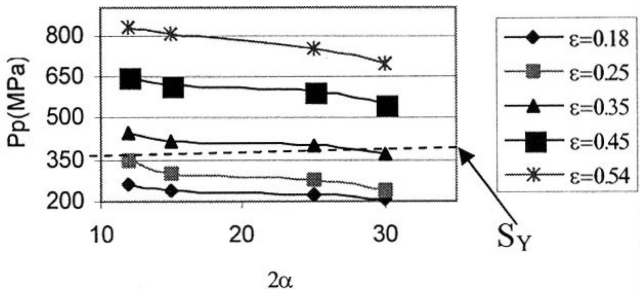

FIGURE 5.—Variation of experimental punch pressure with die angle at different strains.

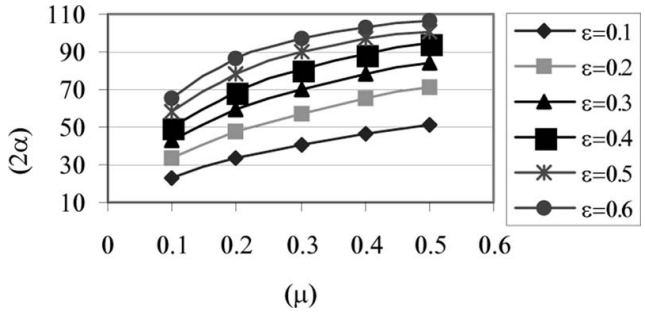

FIGURE 6.—Variation of theoretical optimum die angle with friction factor at different strains.

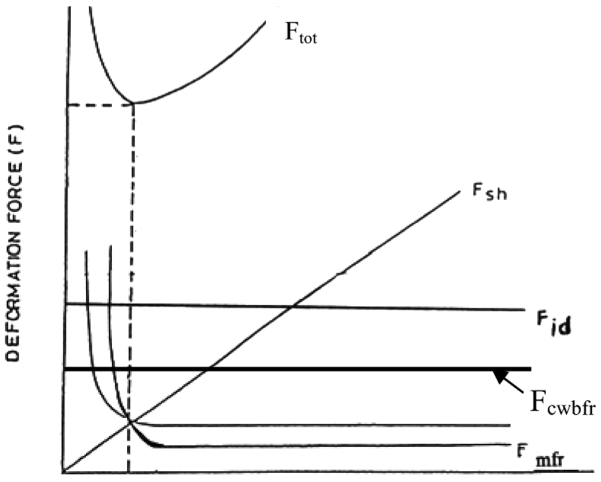

FIGURE 7.—Variation of individual force component with die angle in conventional extrusion.

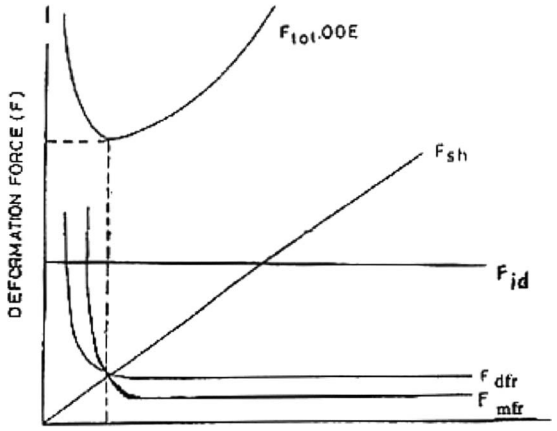

FIGURE 8.—Variation of individual force component with die angle in containerless extrusion.

TABLE 3.—Values of trigonometric functions used in calculation of forces.

α (radians)	0	$\frac{\pi}{4}$	$\frac{\pi}{2}$	$\frac{3\pi}{4}$	π
α (degrees)	0	45	90	135	180
$\tan\alpha$	0	1	∞	-1	0
2α (radians)	0	$\frac{\pi}{2}$	π	$\frac{3\pi}{2}$	2π
2α (degrees)	0	90	180	270	360
$\sin 2\alpha$	0	1	0	-1	0

TABLE 4.—Individual force components.

Force component	Conventional tube extrusion	Containerless tube extrusion
Ideal	$A_0\sigma_{\text{fm}}\varepsilon$	$A_0\sigma_m\varepsilon$
Shear	$A_0(\alpha/2)\sigma_{\text{fm}}$	$A_0(\alpha/2)\sigma_{\text{fm}}$
Die friction	$A_0(2\mu/\sin 2\alpha)\sigma_{\text{fm}}\varepsilon$	$A_0(2\mu/\sin 2\alpha)\sigma_{\text{fm}}\varepsilon$
Mandrel friction	$A_f(2\mu/\tan\alpha)\sigma_{\text{fm}}\varepsilon$	$A_f(2\mu/\tan\alpha)\sigma_{\text{fm}}\varepsilon$
Container wall billet friction	$\mu 2\pi RL\sigma_{\text{fm}}$	absent

TABLE 5.—Temperature rise in deformation zone during deformation.

ΔT_{ad}	$(\beta\sigma_{\text{fm}}\varepsilon)/\rho c$
ΔT_{sh}	$\sigma_{\text{fm}}(\alpha/2)(1/\rho)(1/c)$
ΔT_{dfr}	$(\mu\sigma_N v_R(\cos\alpha)(\Delta t)A)/\rho cV$
ΔT_{mfr}	$\sigma_{\text{fm}}(\mu/\tan\alpha)(1/\rho)(1/c)(A_f/A_0)$

Equation 2 is obtained by differentiating Eq. (1) and equating to zero. It is found that optimum angle depends only on extrusion strain and friction factor. This is shown in Fig 6. In our experiments the friction factor is constant. Therefore, as strain increases the optimum angle should also increase. It is seen clearly from Figs. 4 and 6 that the angle shifts from 25 to 30 as strain varies form 0.18 to 0.54 at a friction factor of 0.14. In Fig. 5 at all strains the minimum punch pressure occurs at an angle of 30°. This is

TABLE 6.—Formulae used in calculations.

σ	$K\varepsilon^n$
σ_{fm}	$((K(\varepsilon)^n)/n+1)$
$\varepsilon_{\text{tube}}$	$\ln(A_0/A_f)=\ln[(d_{0\text{B}}^2-d_{i\text{B}}^2)/(d_{0\text{E}}^2-d_{i\text{E}}^2)]$ (Since $d_{i\text{B}}=d_{i\text{E}}=10$ mm)
$\varepsilon_{\text{tube}}$	$\ln[(d_{0\text{B}}^2-10^2)/(d_{0\text{E}}^2-10^2)]$
Theoretical punch pressure	
$P_{\text{P}_{\text{tube}}}$	$\sigma_{\text{fm}}[\alpha/2+\varepsilon(1+(2\mu/\sin 2\alpha)+(A_f/A_0)(\mu/\tan\alpha))]$
Experimental punch pressure	
$P_{\text{P}_{\text{tube}}}$	F/A_0, $A_0=\pi(d_{o\text{B}}^2-10^2)/4$
Theoretical limit strain	
$\varepsilon_{\text{L}_{\text{Tube}}}$	$[(S_y/\sigma_{\text{fm}})-(\alpha/2)]/[1+(2\mu/\sin 2\alpha)+(A_f/A_0)(\mu/\tan\alpha)]$

expected to be the optimum angle. As the experiments were not carried out at higher angles it cannot be definitely said to be so. But the trend from theoretical curves indicates this. The reason for an optimum angle to occur can be understood from Figs. 7 and 8 in which the individual force component variation with die angle is given. The variation of trigonometric values of $\sin 2\alpha$ and $\tan\alpha$ as a function of α from 0° to 90° is given in Table 3.

The overall force equation for container and containerless extrusion are as follows:

$$F_{\text{Conv.E}} = F_{\text{id}} + F_{\text{sh}} + F_{\text{dfr}} + F_{\text{mfr}} + F_{\text{cwbfr}} \tag{3}$$

$$F_{\text{Contl.E}} = F_{\text{id}} + F_{\text{sh}} + F_{\text{dfr}} + F_{\text{mfr}} \tag{4}$$

The individual force components are given in Table 4.

Theoretical punch pressures are greater than experimental punch pressures. This is explained by the reduced flow stress of the material during deformation due to temperature rise in the deformation zone, as a consequence of adiabatic, frictional, and shear heating. The expressions are given in Table 5. The temperature rise in deformation of CP titanium is high and substantial due to its low specific heat and low density. In the present case coaxial stainless steel sheathed chromel–alumel thermocouples were used to measure the rise in temperature during deformation and it was found to be as high as 145°.

CONCLUSIONS

Optimum angle calculated theoretically depends on extrusion strain and friction factor only. Expected experimental optimum angle is approximately 30° for all extrusion strains at a constant friction factor of 0.14, for commercially pure titanium. Theoretical punch pressure is greater than experimental punch pressure and theoretical limit strain is less than experimental limit strain, at an optimum angle. It can be explained by the temperature rise in the deformation zone due to frictional, shear, and adiabatic heating. Extrusions have to be done at higher angles so as to be sure about the optimum angle. We are planning to carry out these further investigations.

References

1. Avitzur, B. *Metal Forming (Processes and Analysis)*; Tata McGraw Hill: New Delhi, 1977; pp. 229–234.
2. Avitzur, B. *Handbook of Metal Forming Processes*; Wiley: New York, 1983; 150–151.
3. Laue, K.; Stenger, H. *Extrusion Processes Machinery Tooling*; ASM, Ohio, 1981; 49–51.
4. Haraarshiedt, K.; Lange, K. *Investigations on Open Die Extrusion of Thick Walled Hollow Cylindrical Work Piece*; Springer-Verlag: Berlin, 1983 (in German).
5. Srinivasan, K.; Venugopal, P. Direct and inverted open die extrusion (ODE) of rods and tubes. J. Materials Processing Technology **2004**, *153–154*, 756–770.
6. Srinivasan, K.; Venugopal, P. Warm open die extrusion of Ti-6Al – 4V. Journal of Materials Processing Technology **1993**, *38*, 265–278.
7. Srinivasan, K.; Venugopal, P. Adiabatic and friction heating in the open die extrusion of solid and hollow bodies. Journal of Materials Processing Technology **1997**, *70*, 170–177.
8. Srinivasan, K.; Venugopal, P. Hardness-stress-strain correlation in open die extrusion–an alternative to visioplasticity. Journal of Materials Processing Technology **1998**, *95*, 185–190.
9. Dieter, G.E.; Bacon, D. *Mechanical Metallurgy*; McGraw-Hill: London, 1998; 625–629.
10. Altan, T.; Oh, S.; Gegel, H. *Metal Forming*; ASM: Ohio, 1995; 208–209.
11. Srinivasan, K.; Venugopal, P. Influence of die angle on containerless extrusion of C.P. titanium rods. MS and T 05 Pittsburgh, USA, Proceedings of 14th International Symposium on Processing and Fabrication of Advanced Materials (PFAM XIV), September, 2005; 539–551.
12. Male, A.T.; Cockroft, M.G. J. of Inst. Met. **1964–65**, *93*, 38–46.
13. Lange, K. *Handbook of Metal Forming*; McGraw-Hill: New York, 1985; 23–25.
14. Channabasappa, S.N.; Srinivasan, K. Open Die Extrusion of Lead Tubes. M.Tech Thesis, NITK, Surathkal, 2003–2004.